Differential pressure experiment to probe hole growth in freely standing polymer films

C. B. Roth, B. G. Nickel, and J. R. Dutcher[a)]
Department of Physics and the Guelph-Waterloo Physics Institute, University of Guelph, Guelph, Ontario, Canada N1G 2W1

K. Dalnoki-Veress
Department of Physics and Astronomy and Brockhouse Institute for Materials Research, McMaster University, Hamilton, Ontario, Canada L8S 4M1

(Received 26 August 2002; accepted 21 January 2003)

We have developed a sensitive experiment which allows the measurement of the growth of holes in thin freely standing polystyrene (PS) films at elevated temperatures. In the experiment, a constant small pressure difference is applied and maintained across the freely standing film, and the formation and growth of holes is detected as a flow of air through the film. From measurements of freely standing PS films for which the glass transition temperature T_g is equal to the bulk value T_g^{bulk}, as well as for films that are sufficiently thin that T_g is 30 °C less than T_g^{bulk}, we find that substantial chain mobility occurs only at temperatures that are comparable to T_g^{bulk}. The results can be interpreted as a shear thinning effect, which is consistent with previous optical microscopy measurements of hole growth in freely standing PS films. © *2003 American Institute of Physics.* [DOI: 10.1063/1.1568541]

I. INTRODUCTION

The mobility of polymer molecules confined to thin films and near a free surface is a very active field of research,[1–28] with significant advances achieved in fundamental understanding and with applications ranging from barrier layers to adhesives to lubricant layers. The mobility of polymer molecules can occur on different length scales, ranging from the size of monomer segments to the overall size of the polymer molecules, which can be characterized by the root-mean-square end-to-end distance R_{EE} of the molecules. Many different experimental techniques have been used to probe molecular motion at different length scales in thin films and the near-surface region of polymers. In general, these experiments are quite challenging because of the small amount of material probed in the experiments. Motion at a segmental length scale, which is associated with the glass transition, is typically probed using calorimetric and thermal expansivity techniques,[1–10] whereas the diffusion of entire molecules, or chain diffusion, has been measured using a variety of established and novel techniques, including fluorescence,[11–13] dynamic secondary ion mass spectrometry,[14–16] optical microscopy,[17–20] scanning probe microscopy,[21–24] particle embedding techniques,[25] and techniques that probe the relaxation of surface roughness.[26–28] All of the chain diffusion measurement techniques are either perturbative in nature, such as due to external perturbations to the sample[14–16,21–23,25,26] or the use of probe molecules,[11,13,16] or the flow is driven by interactions inherent to the sample geometry or because of the nonequilibrium nature of the sample.[17–20,27,28] The chain diffusion experiments probe either the diffusion parallel to the film plane,[11,13,26–28] or the diffusion perpendicular to the film plane.[12,14–23,25] For very thin polystyrene (PS) films, it is found that the chain diffusion dynamics perpendicular to the film plane are slower or unchanged compared with that in bulk, and the chain diffusion dynamics parallel to the film plane can also become slower.[11] The slowing of the dynamics on the length scale of the overall size of the molecules has to be reconciled with measurements of mobility at the segmental length scale, which invariably show faster dynamics, i.e., lower glass transition temperatures, for very thin PS films. The reconciliation of these data requires behavior that differs from that in bulk, e.g., different mobilities on different length scales or a variation of the segmental mobility across the thickness of the film. The determination of the differences between thin film and bulk dynamics is an important and unresolved issue in polymer physics.

Most thin polymer film chain diffusion measurements have been performed on films supported on substrates.[11,13–15,17,21–23,25–28] The presence of the substrate can add an additional complication because of physical and chemical interactions between the polymer and substrate that can enhance or inhibit chain diffusion. To reduce the additional complications produced by the presence of an underlying substrate, it is possible to use experimental techniques that probe only the near-surface region of relatively thick films.[14,15,21–23,25,28] Alternatively, the underlying substrate can be removed to create unsupported or freely standing films. The freely standing film geometry is appealing for studies of the influence of confinement on the dynamics of polymer molecules because it provides a simplified sample geometry corresponding to one-dimensional confinement which is symmetric about the midplane of the film and free

a)Author to whom correspondence should be addressed; electronic mail: dutcher@physics.uoguelph.ca

from the influence of physical and chemical interactions with an underlying substrate. The freely standing film geometry is also interesting because of the observation of dramatic reductions in the glass transition temperature T_g of freely standing PS films relative to the bulk value of T_g^{bulk} for films with thicknesses h comparable to or less than R_{EE}.[2,6,8] The T_g reductions observed for freely standing PS films are striking for two reasons: first, they are much larger than those measured for supported PS films, and second, they depend substantially on the molecular weight of the polymer,[4,6,8] suggesting that chain confinement is an important contribution to the glass transition dynamics of freely standing films. Measurements of chain diffusion dynamics are therefore important to check if corresponding anomalies also exist in large scale motion of the polymer molecules.

Chain diffusion dynamics were first measured in thin, freely standing PS films by observation of the formation and growth of holes in the films using optical microscopy.[20] At temperatures comparable to or greater than T_g^{bulk}, the freely standing films are unstable to the formation of holes which form either by nucleation at defects such as dust or density inhomogeneities, or spontaneously by thermal fluctuation of the film surfaces.[29] As the holes grow, driven by surface tension, the polymer chains must necessarily move, and the hole growth measurements provide a probe of chain diffusion near the edge of the hole.[20] In the optical microscopy experiments, high molecular weight ($M_w = 767 \times 10^3$) PS molecules were confined to films with thicknesses 96 nm $< h <$ 370 nm, for which $T_g = T_g^{\text{bulk}} = 97\,^\circ\text{C}$, and hole growth was measured at a fixed temperature of $T = 115\,^\circ\text{C}$ which is substantially larger than T_g^{bulk}. In this experiment, as in previous experiments performed on relatively thick ($h > 5\ \mu\text{m}$) polydimethylsiloxane freely standing films,[18,19] the growth of a single hole was measured for each film, and it was found that the hole radius R grew exponentially with time, $R = R_0 e^{t/\tau}$, where τ is the characteristic growth time. Exponential growth of the hole radius is expected for viscous films.[18,19] For the freely standing PS films, it was found that τ decreased with decreasing film thickness h. This result was interpreted in terms of the bulk phenomenon of shear thinning,[30] in which the film viscosity at the edge of the hole, $\eta = \tau\epsilon/h$, where ϵ is the surface tension, decreased with increasing shear strain rate $\dot{\gamma} = 2/\tau$, according to a power law dependence $\eta \sim |\dot{\gamma}|^{-d}$ with $d = 0.65 \pm 0.03$. A challenging aspect of this experiment for very thin films was to quickly identify, using the optical microscope, the formation of a hole somewhere on the relatively large surface area ($\approx 12\ \text{mm}^2$) of the film such that its growth could be measured over a substantial range of radii before substantial thickening of the film occurred.

In the present article, we study hole formation and growth for freely standing PS films that have the bulk value of the glass transition temperature T_g^{bulk}, as well as for very thin freely standing PS films for which the glass transition temperature T_g has been measured to be substantially less than T_g^{bulk}. In particular, it is interesting to ask the following questions: what is the temperature corresponding to substantial chain mobility, as evidenced by measurable hole formation and growth, and how does this temperature compare with the T_g value of the film? There are difficulties associated with the use of optical microscopy to answer these questions. In particular, to probe the onset of hole formation, it is necessary to perform the measurements at lower temperatures for which the time scale of the experiment becomes necessarily very long. It becomes very difficult to observe the formation of individual holes on such a long time scale.

To avoid the disadvantages associated with using optical microscopy to study hole growth in very thin, freely standing PS films at relatively low temperatures, we have developed and used a sensitive differential pressure experiment (DPE). The concept of the DPE is similar to that used previously to study the room-temperature mechanical properties of thin plates and membranes,[31,32] in which the Young's modulus of the films was inferred from measurements of the film deflection at the center of the film as a function of a relatively large applied pressure difference (typically 10 kPa). A similar apparatus has also been used to characterize the room-temperature elastic properties of freely standing membranes of cross-linked monolayers of polyisoprenes.[33] In the present experiment, we apply a small, constant pressure difference (typically 7 Pa), and track the flow of gas through freely standing PS films held at elevated temperatures as holes form and grow in the films due to their inherent thermal instability. Using the DPE, we have measured hole formation and growth in freely standing PS films that are sufficiently thick ($h \approx 90$ nm) such that $T_g = T_g^{\text{bulk}}$, as well as in freely standing PS films that are sufficiently thin ($h \approx 70$ nm) such that T_g is significantly reduced (by 30 °C) from T_g^{bulk}. We find that appreciable hole formation occurs only at temperatures that are comparable to the bulk value of T_g, which is much higher than the T_g value for very thin freely standing PS films. The preliminary results of these measurements indicate that the mobility of confined polymer molecules differs substantially on different length scales, perhaps due to a variation in segmental mobility across the thickness of the films.

Following a description of the preparation of the freely standing PS films, we describe the technical details of the DPE, together with a mathematical analysis of the experiment. The experimental procedure is then described, and representative data, collected at different temperatures for films with both bulk and reduced values of T_g, are presented and discussed.

II. EXPERIMENTAL TECHNIQUES

A. Sample preparation

Monodisperse ($\bar{M}_w/\bar{M}_n = 1.11$), high molecular weight ($\bar{M}_w = 2240 \times 10^3$) PS obtained from Polymer Source Inc. was dissolved in toluene. PS films were deposited by spin-coating dilute solutions (1.2% and 1.5% PS by mass) at 4000 rpm onto freshly cleaved mica. The PS films on mica were annealed under vacuum at $T = 115\,^\circ\text{C}$ for 12 h to remove residual solvent and cooled at 1 °C/min to room temperature. Freely standing PS films were created by using a water transfer technique to place the PS films over a 4-mm-diam hole in a 1 cm^2 stainless steel holder.[8] Pieces of the same PS films were also transferred onto clean Si wafers for a determination of the initial PS film thickness, accurate to within

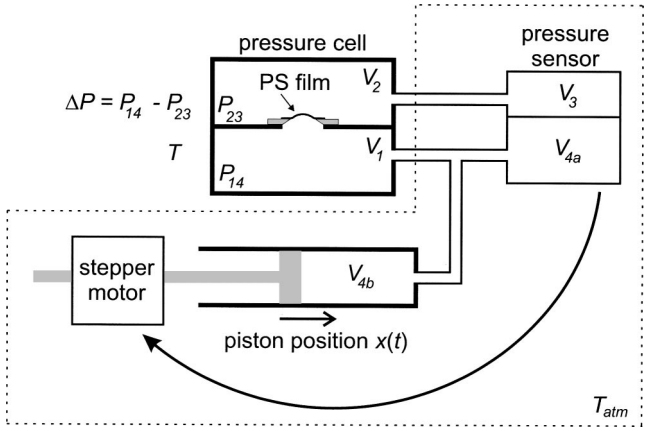

FIG. 1. Schematic diagram of the differential pressure experiment (DPE) identifying the different pressures, volumes and temperatures within the experiment.

± 1 nm, using ellipsometry. Prior to each run of the DPE, the PS films were examined using optical microscopy to ensure that there were not any preexisting holes or tears, which would degrade or prevent the DPE measurement. For the present study, the DPE has been used to study 33 different freely standing PS films of two different nominal thicknesses: 68 ± 1 nm and 91 ± 3 nm.

B. Differential pressure experiment description and procedures

We have developed a sensitive differential pressure experiment which allows a very small pressure difference to be applied and maintained across a freely standing PS film while the film is held at an elevated temperature. A schematic diagram of the experiment is shown in Fig. 1. The heart of the experiment is a thin-walled metal pressure cell, which consists of two compartments of nearly equal volume that are connected via a 4-mm-diam hole (see Fig. 2). The pressure cell is heated using a flexible Kapton heater strip (Omega) which is wrapped around the outside of the pressure cell and located symmetrically with respect to the hole between the compartments of the pressure cell. The PS film, which is freely standing across a 4-mm-diam hole in a 1 cm^2 stainless steel washer, is placed across the hole between the cell compartments, providing a barrier to gas flow, and allowing a pressure difference to exist, between the two compartments. The pressure cell also has a large glass window to allow viewing of the PS film during the experiment. The pressure difference ΔP between the two compartments of the pressure cell is monitored using a sensitive differential pressure transducer (MKS Baratron 223B Pressure Transducer) which has a resolution of 0.13 Pa. The absolute pressure in the lower compartment of the pressure cell is adjusted using a stepper-motor-controlled piston (a glass syringe with a volume of 30 cm^3) connected to this compartment. Each microstep of the stepper motor corresponds to 0.1 μm motion of the piston. During the experiment, the upper compartment of the pressure cell is isolated with respect to atmospheric pressure, allowing the pressure difference across the PS film to be actively stabilized by controlling the pressure in the lower compartment of the pressure cell. The pressure feedback system consists of the differential pressure sensor, the piston and the stepper motor which is computer controlled via a Keithley DAS-1602 data acquisition card. Polyethylene tubing (1/4 in. o. d.) with brass connectors and Swagelok valves is used to connect the pressure cell, piston and differential pressure sensor.

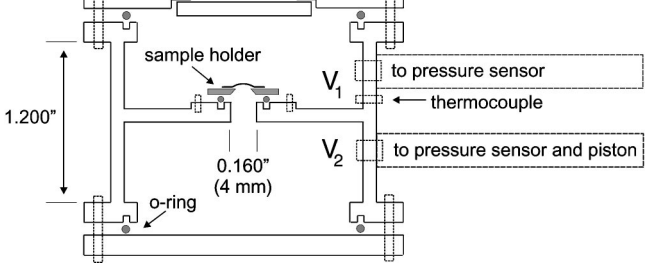

FIG. 2. Simplified technical drawing of cross-sectional view of pressure cell.

In the experiment, the pressure cell is heated quickly at a rate of 5 °C/min to a fixed elevated temperature T with both compartments of the pressure cell open to atmospheric pressure. At the fixed elevated temperature, the system is isolated with respect to atmospheric pressure, and a very small, constant pressure difference (ΔP typically 6.6 Pa$\sim 10^{-4}$ atm) is maintained across the PS film. The temperature of the pressure cell, and therefore of the PS film, is controlled to within ± 0.1 °C using a Eurotherm 808 digital temperature controller with an iron–constantan (type J) thermocouple. The thermocouple junction is bolted directly onto the stainless steel sample holder, and a long length (~ 1 m) of thermocouple wire (36 gauge) is coiled inside the pressure cell to ensure proper measurement of the sample temperature. To isolate the system from slight variations in room temperature, we have enclosed the DPE, with the exception of the pressure cell, in a thermally insulated box which is heated to and maintained at $T_{atm} \sim 30$ °C (see Fig. 1). For each run of the DPE, we fix the temperature T of the pressure cell and the small pressure difference ΔP across the polymer film, and simply track the position of the stepper-motor-controlled piston x as a function of time. The uncertainty in x is determined by the mechanical backlash in the screw thread used to drive the piston and we estimate this to be approximately 1 μm.

C. Analysis of differential pressure experiment

In the differential pressure experiment (DPE), the formation and growth of holes in the freely standing polymer films is detected as a large, monotonic drift in the piston position. The piston drift occurs because the pressure feedback loop maintains a constant small pressure difference ΔP across the film in the presence of the holes, which results in air flow through the holes from the lower compartment to the upper compartment of the pressure cell (see Fig. 1). In this section, we derive an analytic expression for the time dependence of the piston position $x(t)$ in terms of ΔP, the characteristic

growth time τ for the holes, and the four distinct volumes and two different temperatures within the DPE.

We begin by applying the equation of state to the gas on both sides of the film. The number of molecules $N_{23}(t)$ in the volumes V_2 and V_3 is given by (for variable names see Fig. 1)

$$N_{23}(t)=P_{23}(t)\left[\frac{V_2}{kT}+\frac{V_3}{kT_{\text{atm}}}\right], \tag{1}$$

where V_2 and V_3 are independent of time and the absolute pressure $P_{23}(t)$ will vary with time t because of the motion of the piston. Similarly, for volumes V_1 and V_4 we have

$$N_{14}(t)=P_{14}(t)\left[\frac{V_1}{kT}+\frac{V_4(t)}{kT_{\text{atm}}}\right], \tag{2}$$

where V_1 is independent of time, but V_4 changes with time because of the movement of the piston to maintain a constant pressure difference ΔP:

$$V_4(t)=V_{4a}+V_{4b}(t)=V_4(0)-A_p x(t), \tag{3}$$

where A_p is the piston cross-sectional area.

The movement of the piston in response to gas flow through the film will increase the pressure throughout the system. We write the time dependence of the pressure $P_{23}(t)$ in volumes V_2 and V_3 as the initial pressure plus a time-dependent increase in pressure $\delta P(t)$: $P_{23}(t)=P_{23}(0)+\delta P(t)$. The corresponding increase in the number of molecules in volumes V_2 and V_3 is given by $N_{23}(t)=N_{23}(0)+\delta N(t)$ where $\delta N(t)$ is total flow of gas across the film in a time interval of duration t. This allows us to rewrite Eq. (1) as

$$\delta P(t)=\frac{\delta N(t)}{\left[\frac{V_2}{kT}+\frac{V_3}{kT_{\text{atm}}}\right]}. \tag{4}$$

As for volumes V_2 and V_3, there is an increase with time in the pressure in volumes V_1 and V_4, $P_{14}(t)=P_{14}(0)+\delta P(t)$, as well as a decrease in the number of molecules $N_{14}(t)=N_{14}(0)-\delta N(t)$. Combining these equations for N_{14} and P_{14}, together with Eqs. (2), (3), and (4), we can solve for $x(t)$:

$$x(t)=\left[\frac{\delta P(t)}{P_{14}(0)+\delta P(t)}\right]\left[\left(\frac{V_1+V_2}{A_p}\right)\frac{T_{\text{atm}}}{T}+\left(\frac{V_3+V_4(0)}{A_p}\right)\right]. \tag{5}$$

To obtain a more useful expression for $x(t)$, we need a detailed expression for $\delta P(t)$ and therefore $\delta N(t)$ [see Eq. (4)]. This requires a detailed analysis of the flow of gas molecules through holes in the film.[34] Gas flow can occur either by effusion, in which the gas molecules pass through the holes without colliding with each other, or by hydrodynamic flow.[35] Effusion is valid in the limit that the hole diameter is less than the mean free path ℓ of the gas molecules which is $\ell=0.3\ \mu$m for nitrogen gas at atmospheric pressure and $T=100\,^{\circ}$C. By considering a typical areal density of holes (1000 holes over the 13 mm^2 sample area), each with a diameter equal to ℓ, we calculate a gas flow through the holes that corresponds to much less than 1 microstep per second for the stepper motor that drives the piston. Since this rate of piston movement is not observable, measurement of piston motion due to gas flow corresponds to gas flow occurring in the hydrodynamic flow regime. For hydrodynamic flow of gas through the ith circular hole, the volume flow rate Q_i is given by[36]

$$Q_i=\frac{\Delta P r_i^3}{3\eta}, \tag{6}$$

where ΔP is the pressure difference across the film, r_i is the radius of the ith hole, and η is the dynamic viscosity. We can express Eq. (6) as the number of gas particles flowing through the ith hole per unit time

$$\frac{dN_i}{dt}=\frac{\Delta P P_{14} r_i^3}{3\eta kT}, \tag{7}$$

where k is Boltzmann's constant and T is the temperature of the molecules.

The total number of molecules $\delta N_i(t)$ passing through the ith hole within a time interval of duration t is given by

$$\delta N_i(t)=\int_{t_i}^{t}\frac{dN_i}{dt'}dt'=\int_{t_i}^{t}\frac{\Delta P P_{14}}{3\eta kT}r_i^3(t')dt'. \tag{8}$$

The radius of each of the n holes is assumed to grow exponentially with time, which is consistent with optical microscopy measurements of hole growth in freely standing PS films[20]

$$r_i(t')=r_{0i}e^{(t'-t_i)/\tau}, \tag{9}$$

where t_i is the time at which the ith hole forms. Typically, we find that there is a substantial delay between the start of the experiment and the formation of holes, with a relatively narrow distribution of hole sizes at the end of the experiment, as measured using optical microscopy. These results suggest that, following some initial delay, the rate at which holes appear initially increases with time and then decreases with time, corresponding to a peaked distribution of t_i values. Physically, the decrease in the rate of hole formation at later times is reasonable for both hole nucleation and spontaneous hole formation: for hole nucleation, eventually holes will have formed at all nucleation sites, e.g., dust; and for spontaneous hole formation, the entire film becomes unstable to hole formation at the same time with a well-defined separation of the holes. In the Results and Discussion section below, we demonstrate that the data fit quality is poor if we assume that all of the holes form at the same time and that the data fit quality is excellent if we assume a Gaussian distribution of hole onset times centered about a mean time t_0 with a width t_w. We also demonstrate explicitly that the distribution of hole onset times extrapolated from the measured distribution of hole sizes at the end of experiment is in excellent quantitative agreement with the Gaussian distribution of hole onset times obtained from the best fit to the $x(t)$ data. Therefore, the assumption of the Gaussian distribution of hole onset times is justified. We make use of the fact that the number of holes in the film is typically quite large to

derive the following expression for the total flow of gas molecules $\delta N(t)$ across the entire film within a time interval of duration t (for details, see the Appendix):

$$\delta N(t) = \frac{\Delta P P_{14} r_0^3 \tau}{18 \eta k T} G, \tag{10}$$

where

$$G = e^{3(t-t_0)/\tau}\ e^{(3t_w/2\tau)^2}\left[\mathrm{erf}\left(\frac{t-t_0}{t_w}+\frac{3t_w}{2\tau}\right) + \mathrm{erf}\left(\frac{t_0}{t_w}-\frac{3t_w}{2\tau}\right)\right]-\left[\mathrm{erf}\left(\frac{t-t_0}{t_w}\right)+\mathrm{erf}\left(\frac{t_0}{t_w}\right)\right] \tag{11}$$

and erf is the standard error function.

By combining Eqs. (4), (5) and (10), we obtain a functional form for the time dependence of the piston position, written in terms of Eq. (11):

$$x(t) = A_1 \times \frac{A_2 G}{P_{14}(0) + A_2 G}, \tag{12}$$

where A_1 and A_2 are scaling constants, and $P_{14}(0)$ is taken to be atmospheric pressure.[37]

The derivation of Eq. (12) was performed with the assumption of a constant ambient temperature T_{atm}. In fact, T_{atm} is controlled in the experiment by enclosing the components of the experimental setup shown within the dashed lines of Fig. 1 in a large, thermally insulating box. We found that it was necessary to heat these components to a fixed temperature $T_{\mathrm{atm}} \sim 30\,^{\circ}\mathrm{C}$ to isolate the system from fluctuations in the room temperature during the course of the experiment. With the present configuration, it is necessary to open the thermally insulated box to begin each experiment. Because of this, there is a small time dependence of the temperature $T_{\mathrm{atm}}(t)$ at the beginning of the experiment as it approaches its set point value. We measure the temperature $T_{\mathrm{atm}}(t)$ inside the thermally insulting box using a LM35 precision temperature sensor for each run of the DPE. We have found that the time dependence of T_{atm} is well described by the empirical form

$$T_{\mathrm{atm}}(t) = T_f\left[1 - \frac{\Delta T}{T_f} e^{-t/t_1}\right], \tag{13}$$

where t_1 is the time constant associated with the time dependence of T_{atm}, $T_f \sim 303$ K is the asymptotic value of T_{atm} at long times and $\Delta T \sim 1$ K ($\ll T_f$) is the total change in T_{atm} during the experiment.

Since $\Delta T/T_f$ is small, we can use the binomial expansion to write Eq. (13) as

$$T_{\mathrm{atm}}^{-1} \approx T_f^{-1}\left[1 + \frac{\Delta T}{T_f} e^{-t/t_1}\right]. \tag{14}$$

By substituting Eq. (14) into Eqs. (1) and (2), it is possible to obtain an expression for the piston position $x(t)$ which is a refinement to Eq. (12) in that it contains an extra term which can be interpreted as a small background signal arising from the time dependence of $T_{\mathrm{atm}}(t)$:

$$x(t) = A_1 \times \frac{A_2 G}{P_{14}(0) + A_2 G} - C_0(1 - e^{-t/t_1}). \tag{15}$$

D. Data fitting procedure

Best fit values of the two parameters C_0 and t_1 describing the background signal [second term on the right hand side of Eq. (15)] were obtained by fitting the initial portion of the data (typically the first 30 min). The values of C_0 and t_1 were then fixed at their best fit values for the remainder of the fitting procedure. Initial guesses were then chosen for the parameters describing the distribution of hole growth onset times, the mean hole onset time t_0 and the width of the hole onset time distribution t_w, based on the shape of the $x(t)$ data: the initial guess for t_0 was taken to be the time at which $x(t)$ deviated substantially from its value at early times, and the initial guess for t_w was taken to be approximately $0.5 \times t_0$. With the values of t_0 and t_w fixed, all of the $x(t)$ data (subject to the condition that $dx/dt < 5$ μm/s as discussed in the Results and Discussion section) were then fit to Eqs. (11) and (15) allowing the remaining three parameters, the characteristic growth time τ, A_1, and A_2, to vary. The final set of best fit parameter values was then obtained by allowing τ, A_1, A_2, t_0 and t_w to vary and fitting all of the $x(t)$ data to Eqs. (11) and (15).

III. RESULTS AND DISCUSSION

After mounting the freely standing PS films in the DPE pressure cell, the films were heated from room temperature up to the measurement temperature T with both sides of the film exposed to atmospheric pressure ($\Delta P = 0$). Small wrinkles formed in the PS film because of the difference in thermal expansion between the PS film and the stainless steel washer. At the fixed measurement temperature, a small pressure difference (typically $\Delta P = 6.6$ Pa $\sim 10^{-4}$ atm) was applied which caused the freely standing film to bow slightly while maintaining the presence of small wrinkles. We observed by eye that, with the film held at the measurement temperature, the wrinkles in the film disappeared with time. The wrinkles took longer to disappear for lower measurement temperatures, as expected because of the increase in the elastic modulus and viscosity with decreasing temperature. For all films, we observed that the wrinkles disappeared before the onset of hole formation was observed as a monotonic drift of the piston position $x(t)$. For example, for a freely standing PS film of thickness $h = 69$ nm held at a sample temperature of $T = 98\,^{\circ}\mathrm{C}$, the wrinkles disappeared after 300 s whereas the peak of the hole onset time distribution occurred at $t_0 = 13\,600$ s and hole growth occurred with a characteristic growth time of $\tau = 11\,700$ s.

A. Piston position data and quality of fits

In Fig. 3(a) is shown a plot of the piston position x as a function of time for a freely standing PS film of thickness $h = 69$ nm that was held at a fixed temperature of $T = 98\,^{\circ}\mathrm{C}$. The data clearly indicate the expected trends: a small drift in x at short times which becomes overwhelmed at later times by the large piston movement associated with the formation and growth of holes. We have chosen to limit the range of data for each data set in terms of the slope of the $x(t)$ values which is a measure of the instantaneous flow of gas across the film and the total hole area at that time. We

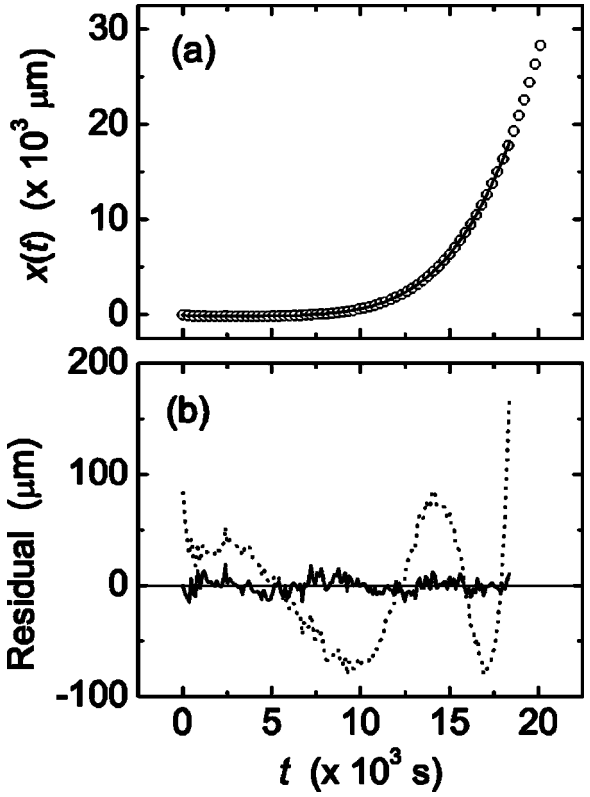

FIG. 3. (a) Piston position x as a function of time for a DPE measurement of a 69-nm-thick freely standing PS film held at $T=98\,^{\circ}\mathrm{C}$. The open circles correspond to data, and the solid line was calculated using Eqs. (11) and (15) with parameters obtained from a least squares fitting procedure: $\tau=11\,700\pm860$ s, $A_1=160\pm60$ mm, $A_2=70.\pm9$ Pa, $t_0=13\,600\pm500$ s, $t_w=5680\pm160$ s, $C_0=147\pm2$ μm, and $t_1=620\pm30$ s. Only every fifth data point is shown such that the quality of the fit can be seen. (b) The residual calculated as the difference between the measured x values and those calculated using Eq. (15) with two different choices of G: Eq. (11) which allows for a Gaussian distribution of hole onset times (solid line); and Eq. (16) which assumes a Dirac delta function distribution of hole onset times for which all holes form at $t=0$ (dotted line).

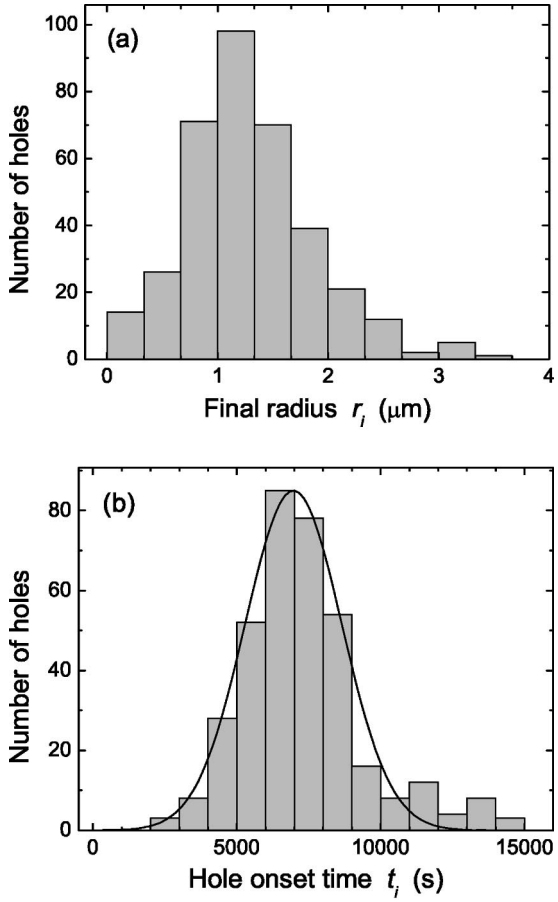

FIG. 4. (a) Distribution of hole radii measured using optical microscopy at the end of the DPE measurement for a freely standing PS film with $h=69$ nm held at $T=99\,^{\circ}\mathrm{C}$. (b) Distribution of hole onset times t_i for the same film as in part (a). For each hole, the onset time t_i was calculated by extrapolating the hole radius measured at the end of the DPE measurement to an initial hole radius of $r_0=0.2$ μm, assuming exponential growth of the hole radius [see Eq. (9)]. The solid curve was calculated using the best fit parameter values of t_0 and t_w obtained from the fit of the $x(t)$ data to Eqs. (11) and (15). The vertical scale of the solid curve was adjusted such that the maximum value of the curve agreed with the maximum value of the hole onset time distribution.

have chosen a cutoff value for the slope of 5 μm/s which is very close to the maximum speed of the piston. For larger slope values, the piston cannot move fast enough to maintain the constant pressure difference ΔP across the film, and the data are therefore unreliable. For the data shown in Fig. 3(a), the range included in the fit corresponds to times $t<18\,000$ s$\sim1.5\tau$. To allow us to critically judge the quality of the fit to the data shown in Fig. 3(a), we have calculated the residual, i.e., the difference between the measured values of x and the values of x calculated using Eqs. (11) and (15) using the best fit parameter values. The calculated residual is shown as a solid line in Fig. 3(b). The residual deviates from zero by only a small amount, with little systematic deviations, indicating an excellent fit to the data over the entire range of times. For comparison, in Fig. 3(b), we also show as a dotted line the residual calculated as the difference between the measured values of x and the values calculated using Eq. (15) and a simplified form for G:

$$G=e^{3(t-t_0)/\tau}-1. \tag{16}$$

Equation (16) corresponds to all of the holes beginning to grow at $t=t_0$ (a Dirac delta function distribution of hole onset times). The residual calculated using Eq. (16) shows much larger, systematic deviations from zero than that calculated using Eq. (11). Therefore the more complicated form for G specified by Eq. (11), which assumes a Gaussian distribution of hole onset times t_i, characterized by a mean hole onset time t_0 and a distribution width t_w, provides a much better fit to the $x(t)$ data.

To test the assumption of a Gaussian distribution for the hole onset times, we have used the following procedure. For a film that was quenched immediately to room temperature at the end of the DPE measurement, we have measured the distribution of hole radii at the end of the experiment using optical microscopy. A typical hole radii distribution is shown in Fig. 4(a) for a freely standing PS film with $h=69$ nm held at $T=99\,^{\circ}\mathrm{C}$. For each hole, we have calculated the hole onset time t_i by extrapolating the hole radius measured at the end of the experiment to an initial hole radius of $r_0=0.2$ μm, assuming that exponential growth of the hole radius has occurred according to Eq. (9). The corresponding distribution of hole onset times for the same film as in part

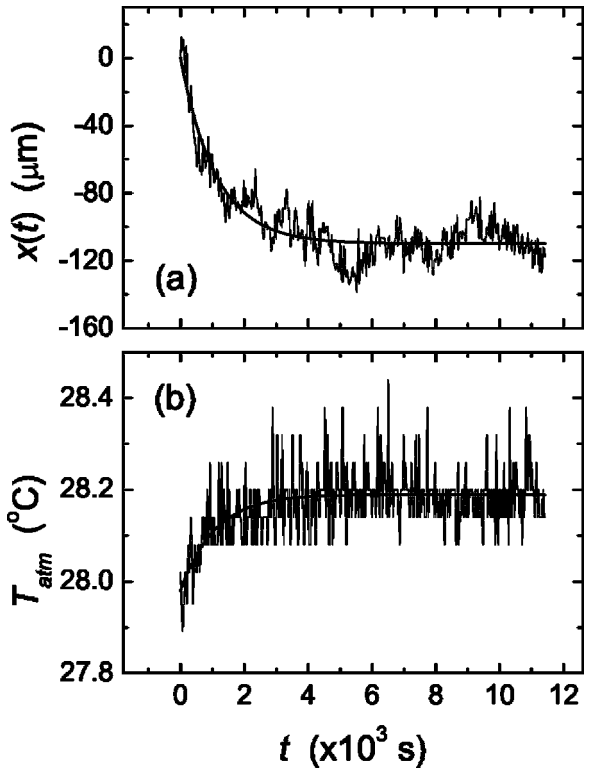

FIG. 5. (a) Piston position x background signal and (b) temperature T_{atm} inside the thermally insulating, temperature-controlled box as a function of time for a metal plate sample placed in the DPE pressure cell. The solid lines are best fits of the data to the second term on the right hand side of Eqs. (15) and (14), respectively. The best fit values of t_1 are 1110 ± 40 s (x background signal) and 1080 ± 170 s (T_{atm} data), which agree within the uncertainty of the t_1 values.

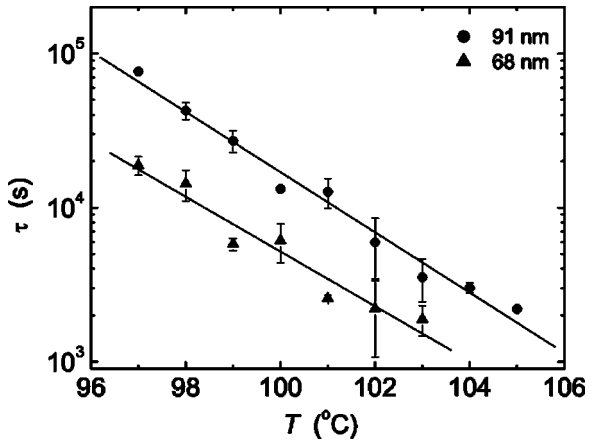

FIG. 6. The characteristic growth time τ vs T for freely standing PS films measured using the DPE. The circles correspond to data obtained for 91 ± 3-nm-thick films that have the bulk value of T_g, and the triangles correspond to data obtained for 68 ± 1-nm-thick films which have T_g values that are reduced by 30 °C from the bulk value. Typically each data point corresponds to the average value of τ measured for two or more films at each film thickness and temperature. The solid curves were calculated using the best fit parameters obtained from linear least squares fits to the $\log(\tau)$ vs T data obtained for each film thickness.

(a) of Fig. 4 is shown in Fig. 4(b), together with a solid curve that was calculated using the best fit parameter values of t_0 and t_w obtained from the fit of the $x(t)$ data to Eqs. (11) and (15). The agreement between the measured and calculated hole onset time distributions is remarkable, and justifies the assumption of a Gaussian distribution for the hole onset times.

To determine the background signal in the DPE, the piston position $x(t)$ was measured in the absence of hole formation and growth by placing a solid metal plate between the two compartments of the pressure cell. In Fig. 5 we show the $x(t)$ background signal and the corresponding $T_{\mathrm{atm}}(t)$ data collected for the solid metal plate sample. We note several important aspects of the background signal shown in Fig. 5(a): (1) the small, initial drift in the background signal is very similar to that measured during the initial stages of a typical DPE measurement of hole formation and growth in freely standing PS films; (2) the overall change in the background signal is small compared with the overall change observed in $x(t)$ during the course of a typical DPE measurement of hole formation and growth in freely standing PS films [see Fig. 3(a)]; and (3) the variations in the background signal after approximately 30 min are very small, indicating that the long term stability of the DPE is excellent. We also note that the variations in the background signal after approximately 30 min are comparable to the variations in the residual calculated using Eqs. (11) and (15) shown in Fig. 3(b), indicating that the fitting function given in Eqs. (11) and (15) provides excellent fits to the $x(t)$ data obtained in the DPE measurements of hole formation and growth in freely standing PS films.

Also shown in Fig. 5 are curves calculated as best fits of the $x(t)$ background signal and the $T_{\mathrm{atm}}(t)$ data to the second term on the right hand side of Eq. (15) and Eq. (13), respectively, which provide excellent fits to each set of data. The best fit values of t_1 are 1110 ± 40 s [$x(t)$ background signal] and 1080 ± 170 s [$T_{\mathrm{atm}}(t)$ data], which agree within the uncertainty of the t_1 values. The initial increase in $T_{\mathrm{atm}}(t)$ occurs because the thermally insulating box is opened briefly at the start of the experiment and $T_{\mathrm{atm}}(t)$ then approaches its set point value which takes approximately 30 min. The close correspondence between the time dependence of the T_{atm} data and the x background signal indicates that the initial deviations of the $x(t)$ background signal from zero are due to $T_{\mathrm{atm}}(t)$. The excellent fit obtained to the $x(t)$ background signal and the close similarity between the small, initial drift in the $x(t)$ background signal and that observed during the hole growth experiments performed using freely standing PS films justifies the use of fitting parameters C_0 and t_1 to describe the initial portion of the $x(t)$ data.

It is important to note that the statistical noise in the $x(t)$ data varies inversely as ΔP. An increase in the signal-to-noise ratio, and therefore a more sensitive measure of the onset of hole formation, could be obtained by increasing ΔP, but this would increase the in-plane stress in the film which could possibly affect the dynamics of hole formation. For the present measurements, we chose ΔP to be as small as possible (typically 7 Pa$\sim10^{-4}$ atm) so as to gently bow the film. We found that doubling ΔP in the DPE resulted in hole growth times that were indistinguishable from those measured using the lower value of ΔP, indicating that in-plane stress effects due to the application of ΔP were not appreciable.

B. Temperature and film thickness dependence of characteristic growth time

We have measured the characteristic growth time τ for holes in 33 different freely standing PS films of two different nominal thicknesses, 68 ± 1 nm and 91 ± 3 nm, held at different temperatures within the range $97\,^{\circ}\mathrm{C}<T<105\,^{\circ}\mathrm{C}$. The measured τ values at different temperatures are plotted in Fig. 6. Measurements were typically performed for several films of the same thickness at the same measurement temperature and the average value of τ for these films is plotted as a single data point in Fig. 6. The solid curves shown in Fig. 6 were calculated using the best fit parameters obtained from linear least squares fits to the $\log(\tau)$ vs T data obtained for each film thickness.

For each film thickness, there is a monotonic decrease in τ with increasing T and, over this limited temperature range, the data are well described by an exponential dependence of τ on T. More significantly, there is a systematic shift between the $\tau(T)$ values obtained for the two film thicknesses. Because of the large difference in the T_g values for films of the two film thicknesses, it is interesting to interpret the shift between the two data sets in Fig. 6 as a shift in temperature. We find that the data obtained for the thinner films, with thicknesses of 68 ± 1 nm, are shifted systematically to lower temperatures by only a small amount ($\sim2.7\,^{\circ}\mathrm{C}$) from the data obtained for the thicker films. The modest temperature shift in the data set for the thinner films is much smaller than the $30\,^{\circ}\mathrm{C}$ reduction in T_g for these films.[8] The small shift between the data sets can be understood in terms of shear thinning,[30] which describes a power law decrease in the film viscosity η with increasing shear strain rate $\dot{\gamma}$, $\eta\sim|\dot{\gamma}|^{-d}$, as in previous hole growth measurements performed at a higher temperature ($T=115\,^{\circ}\mathrm{C}$).[20] The present results, which show a factor of ~3.8 decrease in τ at $T=100\,^{\circ}\mathrm{C}$ as the film thickness is decreased from 91 to 68 nm (by a factor of 1.3), correspond to a decrease in film viscosity with increasing shear strain rate with a value of d which is consistent with that found previously[20] to within the sample-to-sample variation of the measured τ values. A detailed analysis of the film thickness and molecular weight dependence of the DPE results is in progress.[38] The observation of only a small shift between the two $\tau(T)$ data sets obtained in the present study, which can be explained on the basis of the bulk phenomenon of shear thinning, is a direct indication that substantial *chain* mobility occurs in very thin, freely standing PS films only at temperatures that are comparable to that in bulk and, in particular, at temperatures which are much larger than the T_g value for the film. This result suggests that there exists a difference between chain and segmental mobility for thin freely standing polymer films, with segmental mobility occurring at much lower temperatures.

ACKNOWLEDGMENTS

The authors thank Dr. Christian Gigault for his help in the development of the DPE. Financial support of the Natural Sciences and Engineering Research Council (NSERC) of Canada is gratefully acknowledged.

APPENDIX

In this Appendix, we derive a useful expression for the total flow of gas $\delta N(t)$ across the entire film within a time interval of duration t for use in Eq. (4). We write $\delta N(t)$ as the sum of the flow contributions from each of the n holes, as specified by Eqs. (8) and (9):

$$\delta N(t)=\sum_{i=1}^{n}\delta N_i(t)=\sum_{i=1}^{n}\int_{t_i}^{t}\frac{\Delta P P_{14}}{3\eta kT}r_{0i}^{3}e^{3(t'-t_i)/\tau}\,dt'. \tag{A1}$$

To evaluate the sum in Eq. (A1), we can rewrite it in terms of the distribution ζ of hole onset times t_i:

$$\sum_{i=1}^{n}=\sum_{t_i=0}^{t}\zeta(t_i). \tag{A2}$$

If we assume that the times t_i at which the holes form have a Gaussian distribution centered about a mean time t_0 with a width specified by t_w, and that there are a large number of holes such that the summation can be replaced by an integral over onset times t_i, we can write

$$\sum_{t_i=0}^{t}\zeta(t_i)\rightarrow\frac{1}{t_w\sqrt{\pi}}\int_0^t dt_i e^{-(t_i-t_0)^2/t_w^2}.$$

We also assume that all of the holes start with the same initial radius r_0. This results in the following expression for the total flow of gas δN:

$$\delta N(t)=\frac{\Delta P P_{14}r_0^3}{3\eta kTt_w\sqrt{\pi}}\int_0^t dt_i e^{-(t_i-t_0)^2/t_w^2}\int_{t_i}^{t}dt' e^{3(t'-t_i)/\tau}. \tag{A3}$$

In Eq. (A3), we have assumed that $P_{14}(t)$ can be approximated as a constant.[39]

The second integral in Eq. (A3) is straightforward to evaluate

$$\int_{t_i}^{t}dt' e^{3(t'-t_i)/\tau}=\frac{\tau}{3}[e^{3(t-t_i)/\tau}-1].$$

Also, if we write $e^{3(t-t_i)/\tau}$ as $e^{3(t-t_0+t_0-t_i)/\tau}$ and let $x=t_i-t_0$, we obtain

$$\delta N(t)=\frac{\Delta P P_{14}r_0^3\tau}{9\eta kTt_w\sqrt{\pi}}\left[e^{3(t-t_0)/\tau}\int_{-t_0}^{t-t_0}dx e^{-x^2/t_w^2}e^{-3x/\tau}-\int_{-t_0}^{t-t_0}dx e^{-x^2/t_w^2}\right]. \tag{A4}$$

On the right hand side of Eq. (A4), we complete the square in the argument of the exponential in the first integral to obtain

$$\delta N(t)=\frac{\Delta P P_{14}r_0^3\tau}{9\eta kTt_w\sqrt{\pi}}\left[e^{3(t-t_0)/\tau}e^{(3t_w/2\tau)^2}\times\int_{-t_0}^{t-t_0}dx e^{-(x/t_w+3t_w/2\tau)^2}-\int_{-t_0}^{t-t_0}dx e^{-x^2/t_w^2}\right]. \tag{A5}$$

In the integrals on the right hand side of Eq. (A5), we break up the limits of integration as follows:

$$\int_{-t_0}^{t-t_0} \rightarrow \int_{0}^{t-t_0} + \int_{-t_0}^{0}.$$

For the second integral on the right hand side of Eq. (A5), the integrand is even in x such that we can write

$$\int_{-t_0}^{0} dx e^{-x^2/t_w^2} = \int_{0}^{t_0} dx e^{-x^2/t_w^2}. \tag{A6}$$

The first integral on the right hand side of Eq. (A5) is more complicated since the integrand is not even in x:

$$\int_{-t_0}^{0} dx e^{-(x/t_w + 3t_w/2\tau)^2} = \int_{0}^{t_0} dx e^{-(x/t_w - 3t_w/2\tau)^2}. \tag{A7}$$

Upon substitution of Eqs. (A6) and (A7) into Eq. (A5), the integrals can be written as standard error functions which are defined as

$$\mathrm{erf}(x) = \frac{2}{\sqrt{\pi}} \int_0^x dt e^{-t^2}.$$

Thus the expression for δN can be written as

$$\delta N(t) = \frac{\Delta P P_{14} r_0^3 \tau}{18 \eta k T} \left\{ e^{3(t-t_0)/\tau} e^{(3t_w/2\tau)^2} \times \left[\mathrm{erf}\left(\frac{t-t_0}{t_w} + \frac{3t_w}{2\tau} \right) + \mathrm{erf}\left(\frac{t_0}{t_w} - \frac{3t_w}{2\tau} \right) \right] - \left[\mathrm{erf}\left(\frac{t-t_0}{t_w} \right) + \mathrm{erf}\left(\frac{t_0}{t_w} \right) \right] \right\} = \frac{\Delta P P_{14} r_0^3 \tau}{18 \eta k T} G, \tag{A8}$$

where G is given by Eq. (11).

[1] J. L. Keddie, R. A. L. Jones, and R. A. Cory, Europhys. Lett. **27**, 59 (1994).
[2] J. A. Forrest, K. Dalnoki-Veress, J. R. Stevens, and J. R. Dutcher, Phys. Rev. Lett. **77**, 2002 (1996); **77**, 4108 (1996).
[3] J. H. van Zanten, W. E. Wallace, and W. L. Wu, Phys. Rev. E **53**, R2053 (1996).
[4] J. A. Forrest, K. Dalnoki-Veress, and J. R. Dutcher, Phys. Rev. E **56**, 5705 (1997).
[5] J. A. Forrest and J. Mattsson, Phys. Rev. E **61**, R53 (2000).
[6] K. Dalnoki-Veress, J. A. Forrest, P.-G. de Gennes, and J. R. Dutcher, J. Phys. IV **10**, Pr7-221 (2000).
[7] J. A. Forrest and R. A. L. Jones, in *Polymer Surfaces, Interfaces and Thin Films*, edited by A. Karim and S. Kumar (World Scientific, Singapore, 2000).
[8] K. Dalnoki-Veress, J. A. Forrest, C. Murray, C. Gigault, and J. R. Dutcher, Phys. Rev. E **63**, 031801 (2001).
[9] S. Kawana and R. A. L. Jones, Phys. Rev. E **63**, 021501 (2001).
[10] J. A. Forrest and K. Dalnoki-Veress, Adv. Colloid Interface Sci. **94**, 167 (2001).
[11] B. Frank, A. P. Gast, T. P. Russell, H. R. Brown, and C. Hawker, Macromolecules **29**, 6531 (1996).
[12] D. B. Hall and J. M. Torkelson, Macromolecules **31**, 8817 (1998).
[13] K. C. Tseng, N. J. Turro, and C. J. Durning, Phys. Rev. E **61**, 1800 (2000).
[14] X. Zheng, M. H. Rafailovich, J. Sokolov, Y. Strzhemechny, S. A. Schwarz, B. B. Sauer, and M. Rubinstein, Phys. Rev. Lett. **79**, 241 (1997).
[15] Y. Pu, M. H. Rafailovich, J. Sokolov, D. Gersappe, T. Peterson, W.-L. Wu, and S. A. Schwarz, Phys. Rev. Lett. **87**, 206101 (2001).
[16] Y. Pu, H. White, M. H. Rafailovich, J. Sokolov, A. Patel, C. White, W.-L. Wu, V. Zaitsev, and S. A. Schwarz, Macromolecules **34**, 8518 (2001).
[17] G. Reiter, Europhys. Lett. **23**, 579 (1993).
[18] G. Debrégeas, P. Martin, and F. Brochard-Wyart, Phys. Rev. Lett. **75**, 3886 (1995).
[19] G. Debrégeas, P.-G. de Gennes, and F. Brochard-Wyart, Science **279**, 1704 (1998).
[20] K. Dalnoki-Veress, B. G. Nickel, C. Roth, and J. R. Dutcher, Phys. Rev. E **59**, 2153 (1999).
[21] J. Hammerschmidt, W. Gladfelter, and G. Haugstad, Macromolecules **32**, 3360 (1999).
[22] S. Ge, Y. Pu, W. Zhang, M. Rafailovich, J. Sokolov, C. Buenviaje, R. Buckmaster, and R. M. Overney, Phys. Rev. Lett. **85**, 2340 (2000).
[23] X. P. Wang, X. Xiao, and O. K. C. Tsui, Macromolecules **34**, 4180 (2001).
[24] V. N. Bliznyuk, H. E. Assender, and G. A. D. Briggs, Macromolecules **35**, 6613 (2002).
[25] V. Zaporojtchenko, T. Strunskus, J. Erichsen, and F. Faupel, Macromolecules **34**, 1125 (2001).
[26] Y. Liu, T. P. Russell, M. G. Samant, J. Stöhr, H. R. Brown, A. Cossy-Favre, and J. Diaz, Macromolecules **30**, 7768 (1997).
[27] M. Hamdorf and D. Johannsmann, J. Chem. Phys. **112**, 4262 (2000).
[28] T. Kerle, Z. Q. Lin, H. C. Kim, and T. P. Russell, Macromolecules **34**, 3484 (2001).
[29] A. Vrij, F. Th. Hesselink, J. Lucassen, and M. Van Den Tempel, Koninkl. Nederl. Academie van Wetenschappen Amsterdam B **73**, 124 (1970).
[30] W. W. Graessley, Adv. Polym. Sci. **16**, 1 (1974).
[31] E. I. Bromley, J. N. Randall, D. C. Flanders, and R. W. Mountain, J. Vac. Sci. Technol. B **1**, 1364 (1983).
[32] M. G. Allen, M. Mehregany, R. T. Howe, and S. D. Senturia, Appl. Phys. Lett. **51**, 241 (1987).
[33] W. A. Goedel and R. Heger, Langmuir **14**, 3470 (1998).
[34] G. Rossi and M. Nulman, J. Appl. Phys. **74**, 5471 (1993).
[35] K. Huang, *Statistical Mechanics*, 2nd ed. (Wiley, New York, 1987).
[36] J. Happel and H. Brenner, *Low Reynolds Number Hydrodynamics* (Martinus Nijhoff, The Hague, 1983).

[37] Actually $P_{14}(0) = P_{\mathrm{atm}} + \Delta P$, but $\Delta P \ll P_{\mathrm{atm}}$ such that $P_{14} = P_{\mathrm{atm}}$ is a very good approximation.
[38] C. B. Roth and J. R. Dutcher (unpublished).
[39] The assumption that $P_{14}(t)$ is a constant is only accurate to within about 30% during the course of the experiment because the movement of the piston decreases the total volume and increases the pressures in the system. However, in the integrand of Eq. (A1), this time dependence of P_{14} is small enough compared with the exponential time dependence of the hole radii that it can be neglected.